Parametric decays of a circularly polarized electromagnetic wave in an electron-positron magnetized plasma

V. Muñoz and L. Gomberoff
Department of Physics, Facultad de Ciencias, Universidad de Chile, Casilla 653, Santiago, Chile
(Received 30 June 1997)

We study the parametric decays of an electromagnetic wave propagating along an external magnetic field in an electron-positron plasma. We include weakly relativistic effects on the particle motions in the wave field and the nonlinear ponderomotive force. We show that there are a number of resonant and nonresonant wave couplings. These include ordinary decay instabilities, in which the pump wave decays into an electroacoustic mode and a sideband wave. There are also nonresonant couplings involving two sideband waves and a nonresonant modulational instability in which the pump wave decays into two sideband modes. Depending on the parameters involved, there is a resonant modulational instability involving a forward-propagating electroacoustic mode and a sideband daughter wave. [S1063-651X(98)04101-4]

PACS number(s): 82.40.Ra, 51.60.+a

I. INTRODUCTION

The nonlinear behavior of an electromagnetic wave propagating along an external magnetic field in an electron-positron plasma has been studied by several authors (see, e.g., [1]). However, most of the effort has been devoted to the study of the possible self-modulation of the waves. The reason lies in the observational fact that radiation emitted from pulsar magnetospheres shows short intensity variations [2–5]. To account for these micropulses, Chian and Kennel [6] proposed a self-modulational instability of the electromagnetic waves. To this end, these authors considered a nonlinear Schrödinger equation whose coefficients were shown to be incorrect [7]. The reason for this is that Chian and Kennel [6] omitted two sources for nonlinearity, namely, harmonic generation and the ponderomotive effects. Kates and Kaup [7], by using a multiple time-space scale perturbation theory, solved the problem consistently. They showed that in a nonmagnetized electron-positron cold plasma, the system is modulationally stable for both linear and circular polarization. When thermal effects are included, the system becomes modulationally unstable in a very narrow frequency region. It has been recently shown that in the ultrarelativistic case the wave can be self-modulated due to relativistic temperatures and phonon damping [8].

Parametric decay of an electromagnetic wave propagating in an unmagnetized plasma has been studied by Gangadhara *et al.* [9]. There, the authors studied only the modulational instability. However, it was recently shown that the treatment of Ref. [9] has several deficiencies. A full study of parametric decays of linearly polarized waves in an electron-positron plasma is given in Ref. [10].

In the case when the plasma is strongly magnetized, Kates and Kaup [11] showed that the plasma is unstable for frequencies below $\omega_p/2$, where $\omega_p^2=4\pi n_0 e^2/m$ is the electron (positron) plasma frequency. Note that the actual plasma frequency of the system is $\sqrt{2}$ times the electron plasma frequency. Recently, fully relativistic thermal effects have been considered, and it has been shown that, in the ultrarelativistic limit, the system is modulationally unstable for $\omega<\sqrt{\eta}\omega_p$, where η is the ratio between the rest energy density and the enthalpy of the system [12].

Here we study the general structure of parametric instabilities of a large amplitude electromagnetic wave propagating along an external magnetic field. We include weakly relativistic effects on the particle motions in the wave field, the ponderomotive force, and nonrelativistic thermal effects. Note that in the case of a circularly polarized wave, which is the case in a magnetized plasma, there is no harmonic generation [7,11].

Thus, in Sec. II, we describe the model. In Sec. III, we derive the nonlinear dispersion relation. In Sec. IV, we study numerically the dispersion relation. In Sec. V, the results are summarized and discussed.

II. MODEL

We assume that the electron-positron plasma is described by the following set of equations:

$$\frac{\partial n_l}{\partial t}=-\vec{\nabla}\cdot(n_l\vec{v}_l), \tag{1}$$

$$\left(\frac{\partial}{\partial t}+\vec{v}_l\cdot\vec{\nabla}\right)(\Gamma_l\vec{v}_l)=\frac{q_l}{m}\left(\vec{E}+\frac{1}{c}\,\vec{v}_l\times\vec{B}\right)-\frac{\gamma KT}{mn_0}\,\vec{\nabla}n_l, \tag{2}$$

$$\vec{\nabla}\cdot\vec{E}=4\pi\rho, \tag{3}$$

$$\vec{\nabla}\times\vec{E}=-\frac{1}{c}\,\frac{\partial\vec{B}}{\partial t}, \tag{4}$$

$$\vec{\nabla}\times\vec{B}=\frac{4\pi}{c}\,\vec{J}+\frac{1}{c}\,\frac{\partial\vec{E}}{\partial t}, \tag{5}$$

$$\vec{J}=\sum_l q_l n_l\vec{v}_l, \tag{6}$$

$$\rho=\sum_l q_l n_l, \tag{7}$$

$$\Gamma_l=\left(1-\frac{\vec{v}_l^{\,2}}{c^2}\right)^{-1/2}, \tag{8}$$

where n_l is the density of each fluid, $\vec{v}_l$ is the bulk velocity of each fluid, $\vec{E}$ and $\vec{B}$ are the electric and magnetic fields, respectively, K is the Boltzmann constant, $\vec{J}$ is the total current, γ is the adiabatic coefficient, T is the common temperature, m is the particle mass, and c is the speed of light.

We assume that a circularly polarized electromagnetic pump wave propagates along the z axis, as well as the existence of a constant magnetic field in the same direction, so that the total zeroth-order electric and magnetic fields are given by

$$\vec{B}_0 = B[\hat{x}\,\cos(k_0 z-\omega_0 t)+\hat{y}\,\sin(k_0 z-\omega_0 t)]+B_{0z}\hat{z}, \quad (9)$$

$$\vec{E}_0 = E[\hat{x}\,\sin(k_0 z-\omega_0 t)-\hat{y}\,\cos(k_0 z-\omega_0 t)], \quad (10)$$

$$B=\frac{ck_0}{\omega_0}E. \quad (11)$$

Adopting the notation for transverse magnitudes

$$A_{\perp 0}=A_{0x}+iA_{0y}=Ae^{i(k_0 z-\omega_0 t)}, \quad A \text{ real}, \quad (12)$$

we find that this wave induces a particle transversal velocity given by

$$v=+\frac{qB}{mck_0}\,\eta\left(1-\frac{\alpha^2}{2}\,\eta^3\right), \quad (13)$$

$$\alpha=\frac{|q|}{mc^2k_0}B, \quad (14)$$

$$\eta=\frac{\omega_0}{\omega_0-\omega_c}, \quad (15)$$

$$\omega_c=\frac{qB}{mc}. \quad (16)$$

In order to obtain the zeroth-order approximation, we have assumed that there is an electromagnetic wave of the form $\exp[i(k_0 z-\omega_0 t)]$. Then the dispersion relation of the electromagnetic wave, including weakly relativistic effects, is given by

$$\omega_0^2=c^2k_0^2+\omega_p^2\sum_j\,\eta_j\left(1-\frac{\alpha^2}{2}\,\eta_j^3\right), \quad (17)$$

where ω_p is the electron plasma frequency, $j=e$ for electrons and $j=p$ for positrons.

Note that the small parameter is α. So since v is proportional to α [see definition (13)], the theory is weakly relativistic and the factor Γ can be expanded around α^2.

In Fig. 1(a), we show the dispersion relation of the pump wave including weakly relativistic effects on the particle motion in the wave field of the pump, Eq. (17). We have chosen $\omega_p/\omega_c=0.5$ and $\alpha=0.01$. The first quadrant corresponds to right-hand polarized waves propagating in the direction of the external magnetic field. The right-hand polarized waves are supported by the positrons and have a resonance at the positron gyrofrequency, $\omega_0=\omega_c$. The second quadrant corresponds to right-hand polarized waves moving in the opposite direction of the external magnetic field. These waves are supported by the electrons and have a resonance at the electron gyrofrequency, $\omega_0=-\omega_c$. The third quadrant corresponds to left-hand polarized waves, moving in the direction of the magnetic field. These waves are supported by the electrons and the branch has a resonance at the electron gyrofrequency. The fourth quadrant corresponds to left-hand polarized waves, moving in the opposite direction to the external magnetic field and supported by the positrons.

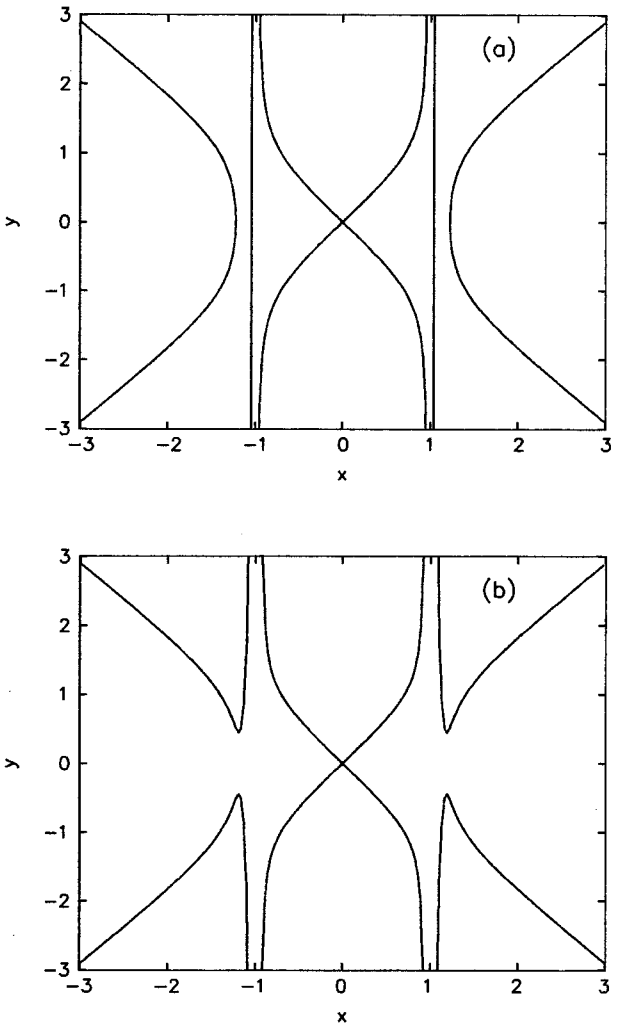

FIG. 1. Dispersion relation of the pump wave, Eq. (17). Normalized wave number $y=k_0c/\omega_c$ vs normalized frequency $x=\omega_0/\omega_c$ for $\omega_p/\omega_c=0.5$. (a) $\alpha=0.01$. (b) $\alpha=0.05$.

As the pump wave intensity increases, there is an instability for frequencies starting at a cutoff frequency $\omega_0>\omega_c$ and $k_0=0$. This is illustrated in Fig. 1(b) for $\alpha=0.05$.

Assuming that the system consists now of electrons, positrons, and a circularly polarized electromagnetic wave satisfying Eq. (17)—the pump wave—we perturb the system again with a perturbation of the form $\exp[i(kz-\omega t)]$. We find the set of equations

$$\frac{\partial}{\partial t}\left[\delta v_\perp\left(1+\frac{v_{\perp 0}v_{\perp 0}^*}{c^2}\right)+\delta v_\perp^*\,\frac{v_{\perp 0}^2}{2c^2}\right]+\delta v_z\,\frac{\partial}{\partial z}\left[v_{\perp 0}\left(1+\frac{1}{2}\,\frac{v_{\perp 0}v_{\perp 0}^*}{c^2}\right)\right]=\frac{q}{m}\left[\delta E_\perp+\frac{i}{c}\,(\delta v_z B_{\perp 0}-\delta v_\perp B_{0z})\right], \quad (18)$$

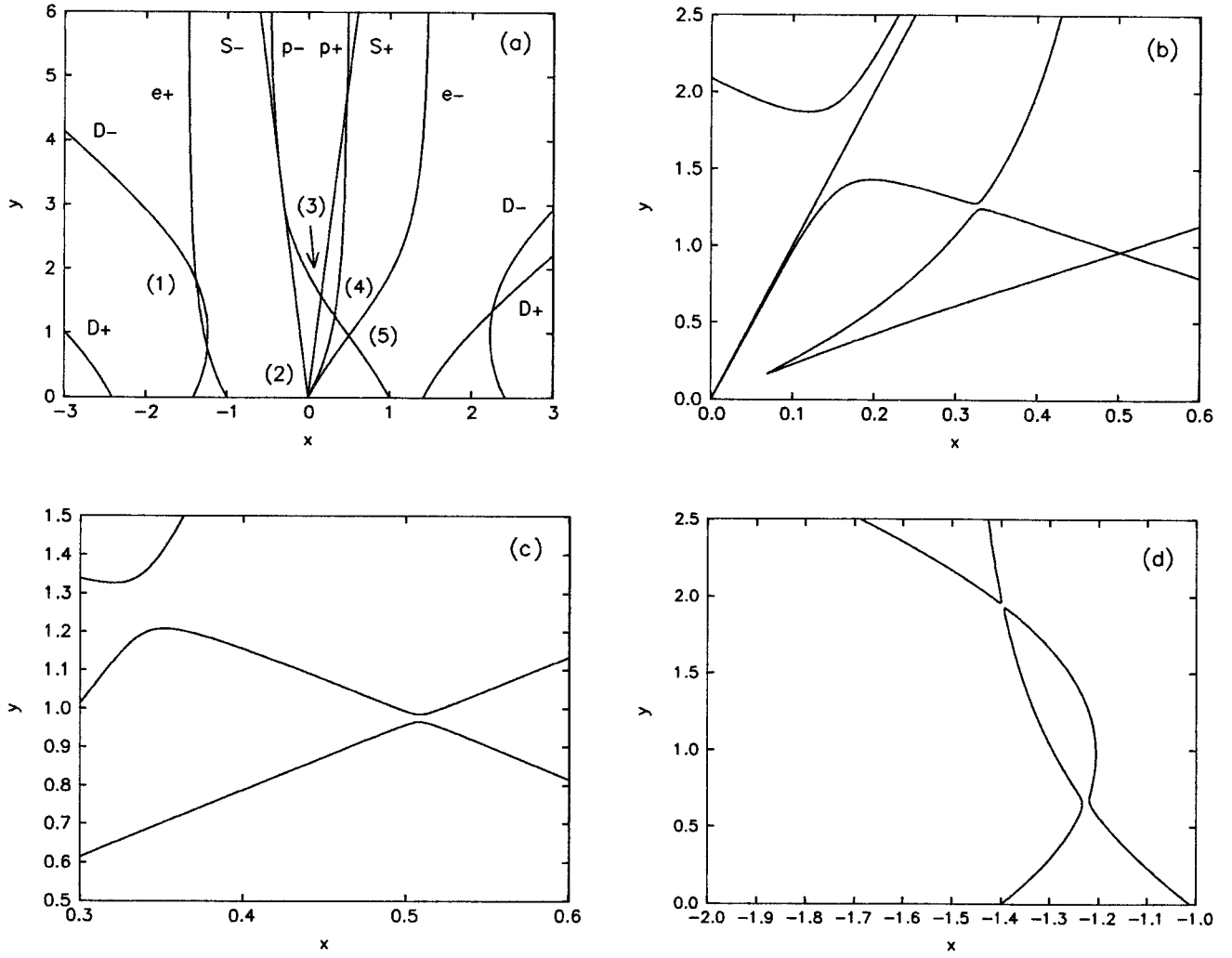

FIG. 2. Nonlinear dispersion relation, Eq. (32). Normalized wave number $y=kc/\omega_c$ vs frequency $x=\omega/\omega_c$ for $\omega_p/\omega_c=1$ and $v_s/c=0.1$. (a) $\alpha=0$. (b) $\alpha=0.1$. (c) $\alpha=0.2$. (d) $\alpha=0.2$, showing the details of the coupling (e_+, D_-).

$$\left[\frac{\partial^2}{\partial t^2}\left(1+\frac{1}{2}\frac{v_{\perp 0}v_{\perp 0}^*}{c^2}\right)-v_s^2\frac{\partial^2}{\partial z^2}\right]\delta v_z$$

$$=\frac{q}{m}\frac{\partial}{\partial t}\left[\delta E_z+\frac{1}{c}\frac{1}{2i}\left(\delta v_\perp^* B_{\perp 0}-\delta v_\perp B_{\perp 0}^*\right.\right.$$

$$\left.\left.+v_{\perp 0}^*\delta B_\perp - v_{\perp 0}\delta B_\perp^*\right)\right], \tag{19}$$

$$\frac{\partial}{\partial z}\,\delta E_z = 4\pi e(\delta n_p-\delta n_e), \tag{20}$$

$$\left(\frac{1}{c^2}\frac{\partial^2}{\partial t^2}-\frac{\partial^2}{\partial z^2}\right)\delta B_\perp = i\,\frac{4\pi e}{c}\frac{\partial}{\partial z}\left[n_0(\delta v_{p\perp}-\delta v_{e\perp})\right.$$

$$\left.+\delta n_p v_{p\perp 0}-\delta n_e v_{e\perp 0}\right]. \tag{21}$$

Longitudinal and transversal perturbations are of the form

$$\delta A_z = \mathrm{Re}[\tilde{A}e^{i(kz-\omega t)}] \tag{22}$$

and

$$\delta A_\perp = a_+ e^{i(k_+ z-\omega_+ t)}+a_- e^{i(k_- z-\omega_- t)}, \tag{23}$$

respectively, with $k_\pm = k_0 \pm k$ and $\omega_\pm = \omega_0 \pm \omega$. From Faraday's law (4) and the continuity equation (1), it follows that

$$e_\pm = -i\,\frac{\omega_\pm}{c}\frac{b_\pm}{k_\pm}, \tag{24}$$

$$\tilde{n} = n_0\,\frac{k\tilde{v}}{\omega}. \tag{25}$$

From the condition of charge quasineutrality,

$$\delta n_p = \delta n_e,$$

and Eq. (25) it follows that

$$\tilde{v}_p = \tilde{v}_e. \tag{26}$$

Using Eqs. (12) (13), and (22)–(26), in Eqs. (18)–(21), we obtain

$$\left[\omega_+(1+\alpha^2\eta^2)-\omega_c\right]v_+ + \left[\omega+\frac{1}{2}\,\alpha^2\eta^2\right]v_-^*$$

$$-\left[\frac{1}{2}\frac{qB}{mc}\frac{\omega_c}{\omega_0}\,\eta\left(1-\frac{1}{2}\,\alpha^2\eta^3\right)\right]\tilde{v} = \frac{q}{mc}\,\omega_+\,\frac{b_+}{k_+}, \tag{27}$$

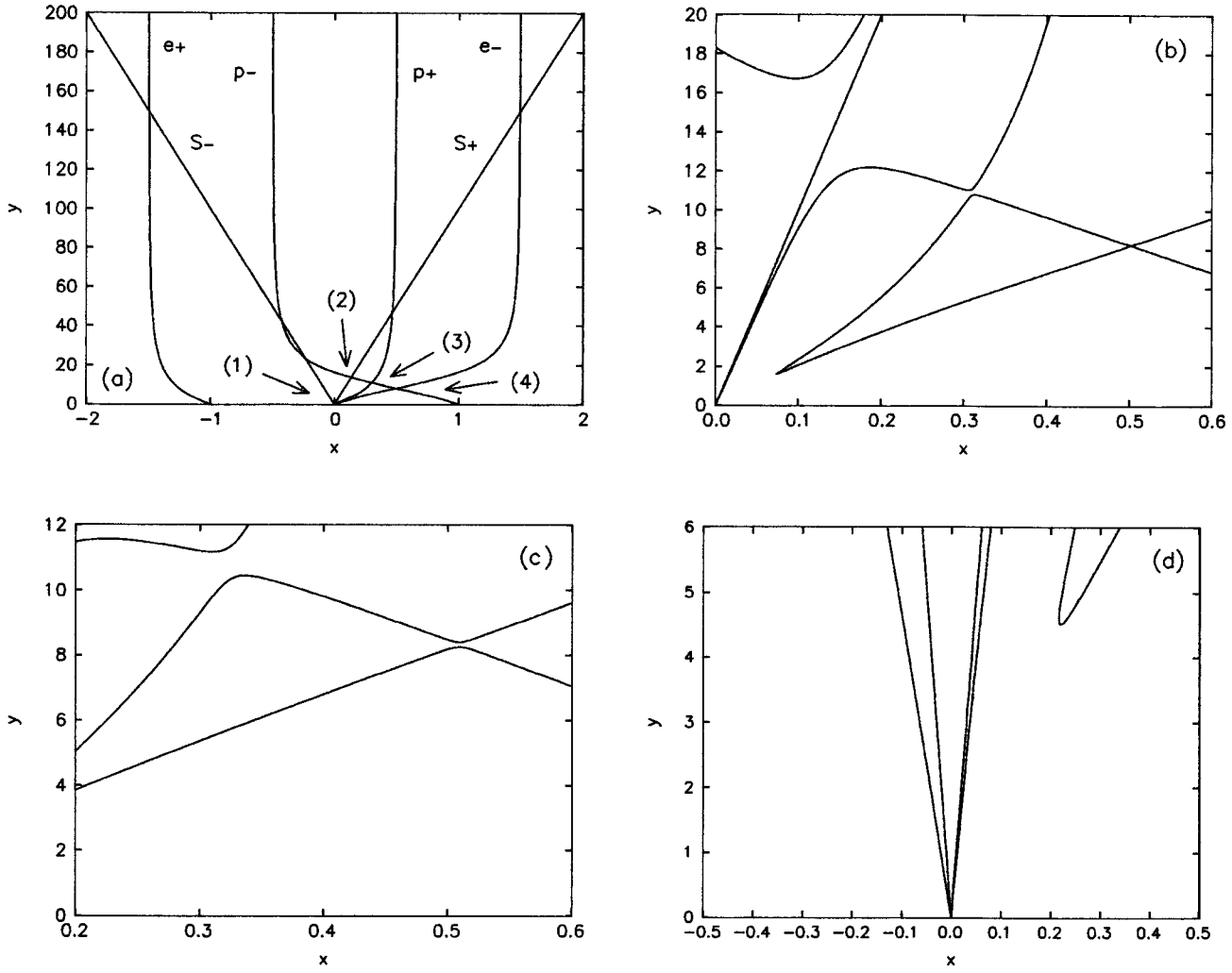

FIG. 3. Nonlinear dispersion relation, Eq. (32). Normalized wave number $y=kc/\omega_c$ vs frequency $x=\omega/\omega_c$ for $\omega_p/\omega_c=10$ and $v_s/c=0.01$. (a) $\alpha=0$. (b) $\alpha=0.01$. (c) $\alpha=0.02$. (d) Enlargement of the origin for $\alpha=0.03$.

$$\left[\omega_- - \frac{1}{2}\,\alpha^2\eta^2\right]v_+ + [\omega_-(1+\alpha^2\eta^2)-\omega_c]v_-^* - \left[\frac{1}{2}\,\frac{qB}{mc}\,\frac{\omega_c}{\omega_0}\,\eta\left(1-\frac{1}{2}\,\alpha^2\eta^3\right)\right]\tilde{v} = \frac{q}{mc}\,\omega_-\,\frac{b_-^*}{k_-}, \tag{28}$$

$$\left[-\omega^2\left(1+\frac{1}{2}\,\alpha^2\eta^2\right)+v_s^2k^2\right]\tilde{v} = \frac{q}{mc}\,\omega\left[B(v_+-v_-^*)+\frac{qB}{mck_0}\,\eta\left(1-\frac{1}{2}\,\alpha^2\eta^3\right)\times(b_-^*-b_+)\right], \tag{29}$$

$$(c^2k_+^2-\omega_+^2)b_+ = -4\pi cek_+n_0\left\{v_{p+}-v_{e+}+\frac{1}{2}\,\frac{k\tilde{v}_p}{\omega}\times\alpha c\left[\eta_p\left(1-\frac{1}{2}\,\alpha^2\eta_p^3\right)+\eta_e\left(1-\frac{1}{2}\,\alpha^2\eta_e^3\right)\right]\right\}, \tag{30}$$

$$(c^2k_-^2-\omega_-^2)b_-^* = -4\pi cek_-n_0\left\{v_{p-}^*-v_{e-}^*+\frac{1}{2}\,\frac{k\tilde{v}_p}{\omega}\,\alpha c\left[\eta_p\left(1-\frac{1}{2}\,\alpha^2\eta_p^3\right)+\eta_e\left(1-\frac{1}{2}\,\alpha^2\eta_e^3\right)\right]\right\}. \tag{31}$$

III. NONLINEAR DISPERSION RELATION

Upon elimination of all quantities $(\tilde{v},v_\pm,b_\pm)$ from Eqs. (27)–(31), we obtain the following nonlinear dispersion relation:

$$0=F_{1+}F_{2-}-F_{2+}F_{1-}, \tag{32}$$

where $F_{1\pm}$ and $F_{2\pm}$ are defined in the Appendix.

When $\alpha=0$, Eq. (32) reduces to

$$0=S_pS_eD_+D_-, \tag{33}$$

where

$$S_p=S_e=\omega^2-v_s^2k^2, \tag{34}$$

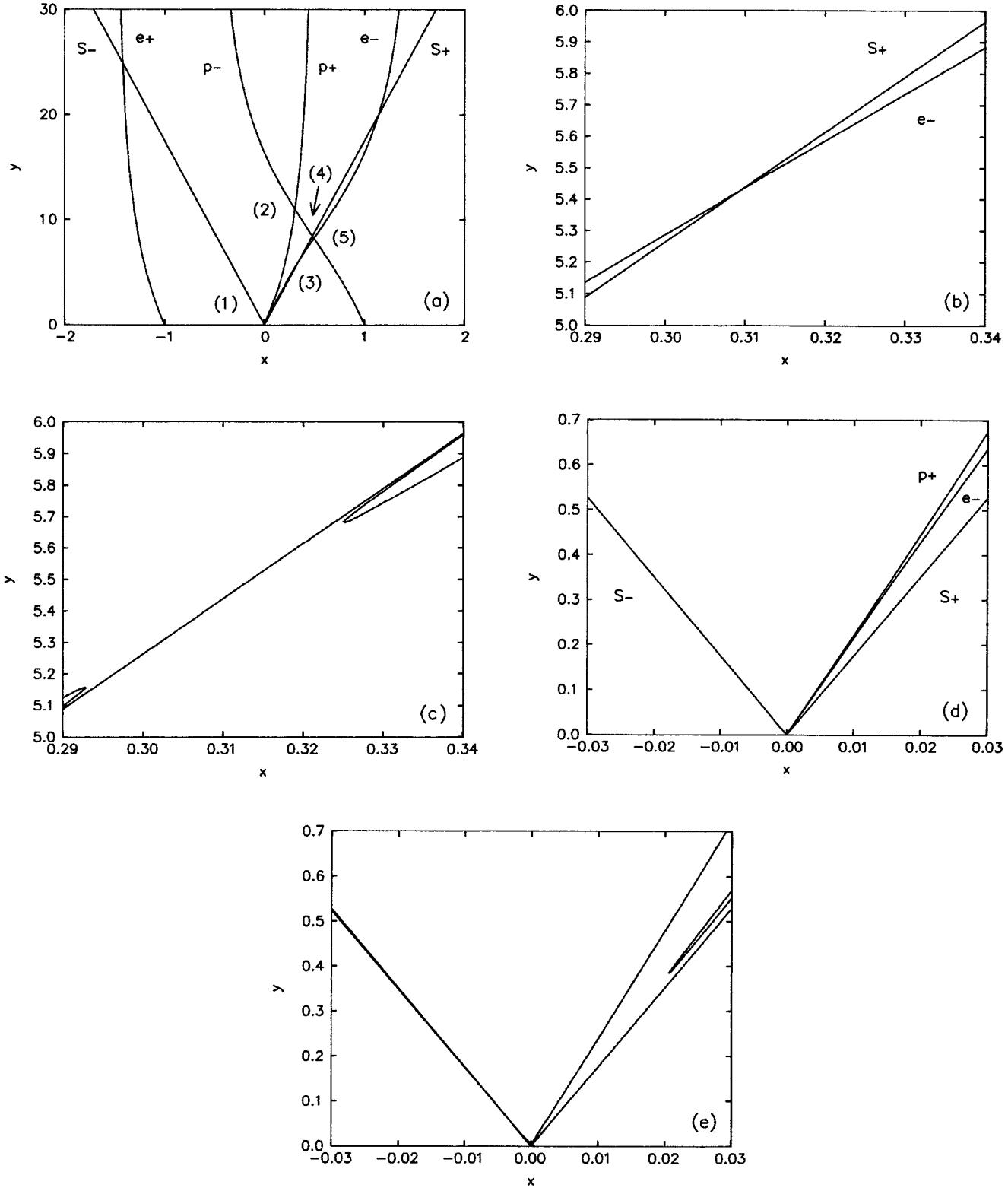

FIG. 4. Same as Fig. 3, for $\omega_p/\omega_c=10$ and $v_s/c=0.057$. (a) $\alpha=0$. (b) The crossing (S_+,e_-) for $\alpha=0$. (c) The same crossing for $\alpha=0.001$. (d) Enlargement of the origin for $\alpha=0$. (e) Same as (d) for $\alpha=0.01$.

$$D_\pm = c^2k_\pm^2 - \omega_\pm^2 + \omega_p^2\left(\frac{\omega_\pm}{\omega_\pm-\omega_{pc}}+\frac{\omega_\pm}{\omega_\pm-\omega_{ec}}\right). \quad (35)$$

The solutions $D_\pm=0$ and $S_p=S_e=0$ correspond to the electromagnetic waves and the electroacoustic modes, respectively. There are four electroacoustic modes, two propagating in the direction of the electromagnetic wave and the other in the opposite direction. When $\alpha\neq 0$, the modes are coupled. A necessary condition for wave coupling is that the resonance conditions must be satisfied, namely, $n\omega_0=\omega_1$

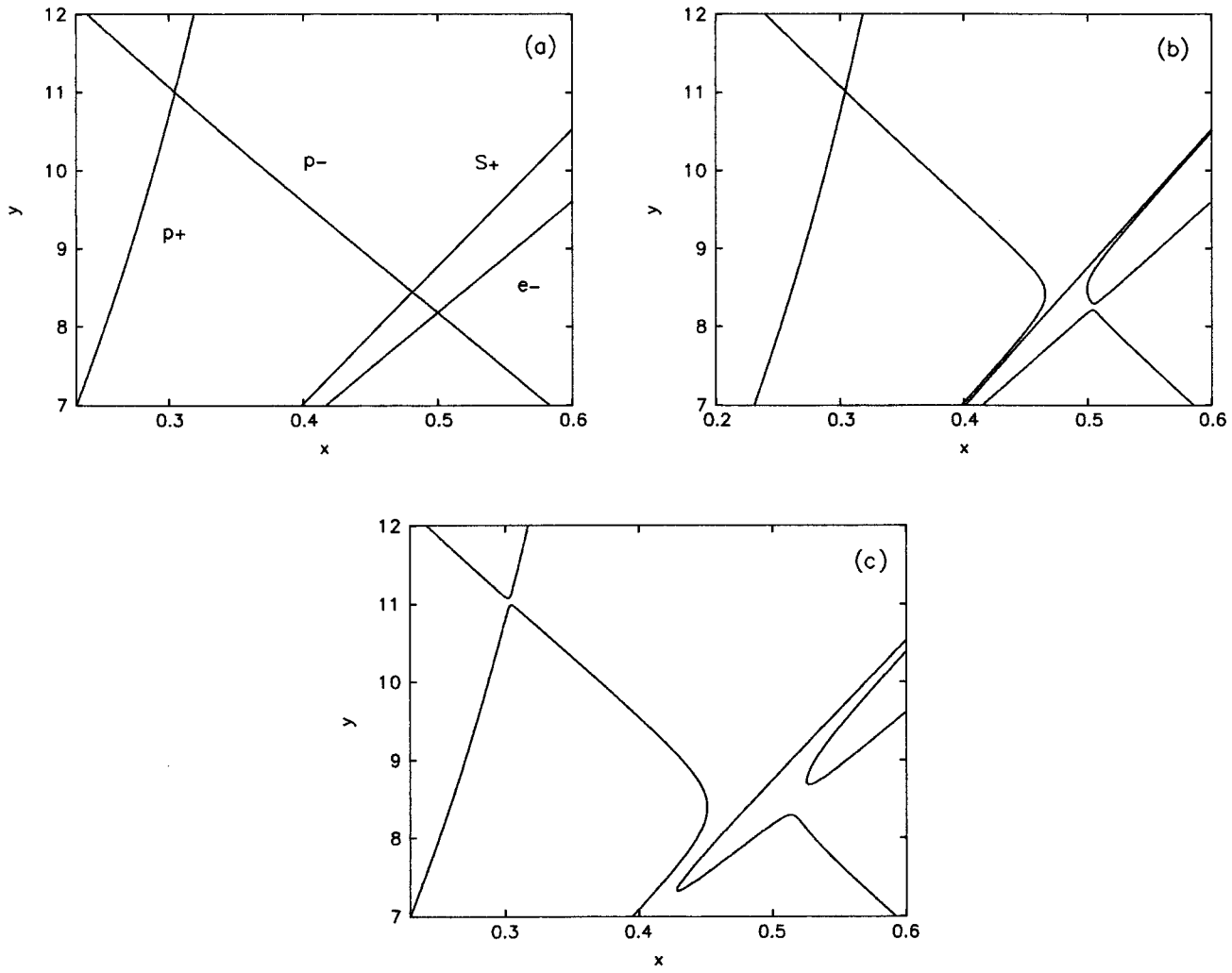

FIG. 5. Same as Fig. 4, showing in details the crossings involving p_-. (a) $\alpha=0$. (b) $\alpha=0.005$. (c) $\alpha=0.01$.

$+\omega_2$ with $n=1,2,3,\ldots$, where ω_1 and ω_2 are the frequencies of the daughter waves [13].

For the case of an unmagnetized plasma ($B_{0z}=0$, $\eta=1$, $\omega_c=0$), Eq. (32) reduces to

$$S[D_+D_- -(D_+ + D_-)\omega_p^2\alpha^2] = -\omega_p^2\alpha^2c^2k^2(1-\alpha^2) \times (D_+ + D_-), \qquad (36)$$

which corresponds to the dispersion relation of circularly polarized electromagnetic waves in an unmagnetized electron-positron plasma [14].

In the next section we solve numerically the nonlinear dispersion relation for various regions in parameter space by using a method first derived by Longtin and Sonnerup [15] (see also [16–19]).

IV. NUMERICAL ANALYSIS OF THE DISPERSION RELATION

We now solve Eq. (32) numerically. To this end, we choose a value of the pump wave frequency, $\omega_0=0.5$, and from Eq. (17) we determine the corresponding wave number y_0 for $\alpha=0$. In Fig. 2(a), we show the solutions of Eq. (32) for $\omega_p/\omega_c=1$, $v_s/c=0.1$, and $\alpha=0$. With these values, $y_0=0.9574$. It is enough to consider the upper half of the (x,y) plane, since the lower half plane is symmetric to reflections through the origin. There are eight lines in the figure corresponding to the eight real solutions of $D_\pm=0$. Four of these lines are parabolic and exhibit no resonance. They are labeled as $D_\pm$ in Fig. 2(a). The lines $p_\pm$ also correspond to solutions of $D_\pm$, but they resonate at the proton gyrofrequency $\omega_\pm=\omega_c$; similarly, $e_\pm$ is the branch of $D_\pm=0$ which resonates at the electron gyrofrequency $\omega_\pm=-\omega_c$. There are also four other lines corresponding to the electroacoustic modes present in the system. These are straight lines passing through the origin and symmetric with respect to the y axis [see Eq. (A15) in the Appendix]. In the case when $\alpha=0$ there are only two such lines because we have assumed equal electron and positron temperatures. However, in the presence of the pump wave, the acoustic modes associated with the electrons and protons separate from each other, giving rise to four lines, two corresponding to acoustic modes propagating in the direction of the pump wave [in Fig. 2(a) they are labeled by S_+ and they overlap] and the other two propagating in the opposite direction (labeled by S_-). From Fig. 2(a), it follows that there are a number of crossings between the solutions of Eq. (32). Some of these crossings can give rise to wave coupling when the pump wave is

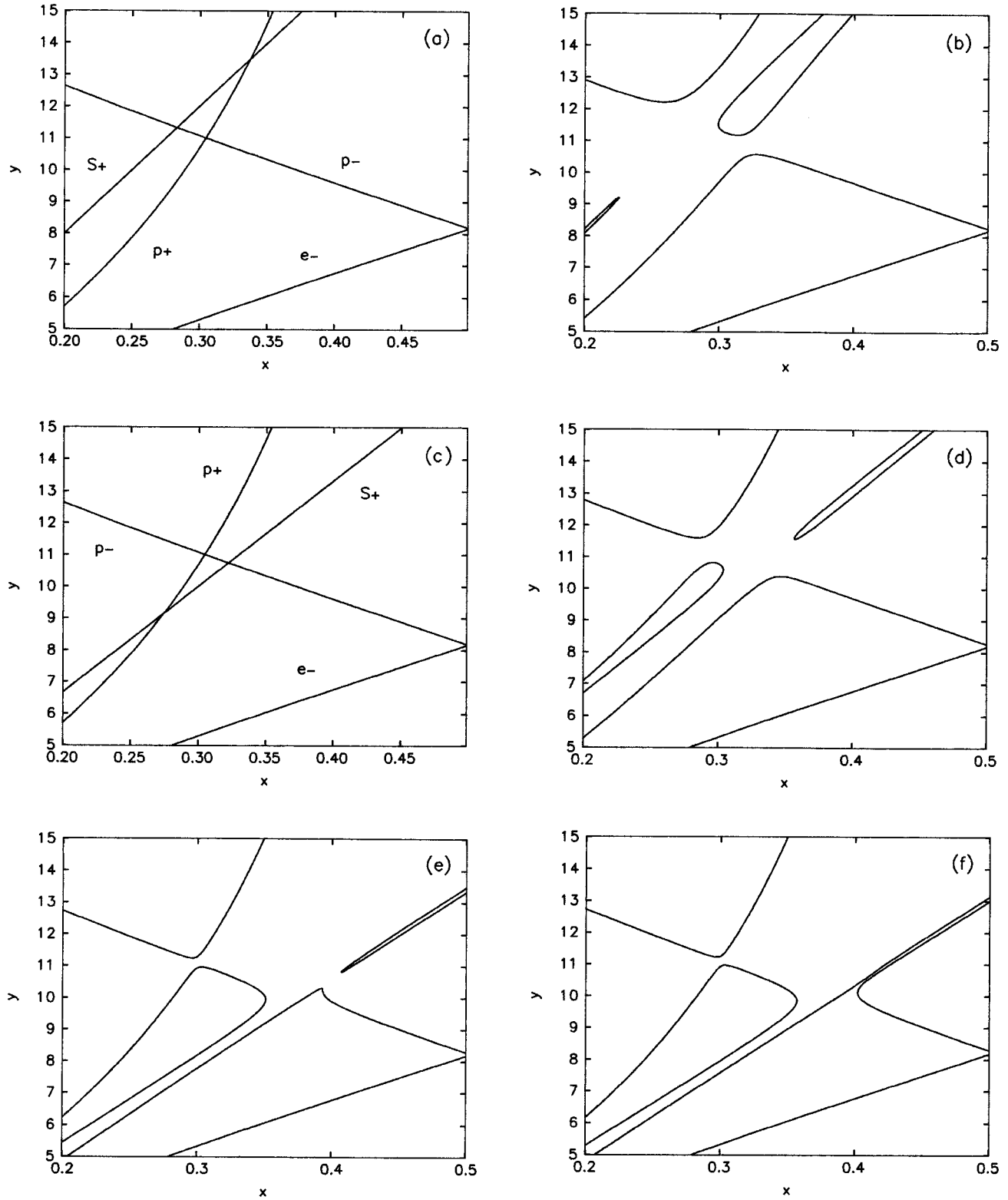

FIG. 6. Same as Fig. 5(a). (a) $v_s/c=0.025$ and $\alpha=0$. (b) Same as (a), $\alpha=0.01$. (c) $v_s/c=0.03$ and $\alpha=0$. (d) Same as (c), but for $\alpha=0.01$. (e) Same as (d), but for $v_s/c=0.037$. (f) Same as (d), but for $v_s/c=0.038$.

switched on. Only crossings between modes satisfying energy conservation can lead to wave coupling. This is a necessary but not a sufficient condition. The crossings leading to wave couplings are labeled from (1) to (5) in Fig. 2(a). Figure 2(a) does not show all the crossings in the upper half of the (x,y) plane. There are two additional crossings, above the displayed portion of the figure, between (S_-,e_+) and (S_+,e_-), but they do not give rise to wave coupling. In Fig. 2(b), we have switched on the pump wave by setting $\alpha=0.1$. We see that some crossings are now gaps. This means that at these crossings we have instabilities, indicating, thereby, wave coupling. From Fig. 2(b), it follows that there are several possible couplings. Starting from the top, there is one corresponding to the crossing of an electroacoustic mode

propagating forward (S_+) and the solution of $D_-=0$, which has a resonance at $\omega_-=\omega_c(p_-)$. We see that the two electroacoustic modes not only separate from each other when $\alpha\neq 0$, but also only one of them couples to p_-. This behavior will be found again later. The crossing with the electroacoustic mode gives rise to an ordinary decay instability, in which the pump wave decays into a forward-propagating electroacoustic mode of frequency ω and a sideband wave of frequency ω_-. The crossing between (p_+,p_-) is a nonresonant coupling in which the pump wave decays into two sideband waves [20]. There is then another nonresonant coupling between two solutions of $D_-=0$ (e_-,p_-), which is more clearly seen in Fig. 2(c) when $\alpha=0.2$. Finally, in Fig. 2(b) there is a crossing at the origin between (p_+,e_-). This crossing gives rise to a gap starting at the origin and corresponds to a nonresonant modulational instability. Figure 2(d) shows the only other coupling for this set of parameters, at the crossing (e_+,D_-).

In Fig. 3(a) we study the case when $\omega_p/\omega_c=10$, $\alpha=0$, and $v_s/c=0.01$. The parabolic branches $D_\pm$ are more separated from each other than they are for $\omega_p=1$, and, therefore, the crossings between (e_+,D_-) have disappeared. The crossing between (D_+,D_-), shown in Fig. 2(a), is still present, but as in the previous case, it does not lead to coupling. Therefore, the lines $D_\pm$ are irrelevant, and we concentrate on the other six lines, as shown in Fig. 3(a). The crossings that lead to wave coupling are labeled from (1) to (4); they are the same as in the previous case [$\omega_p=1$, Fig. 2(a)]. In Fig. 3(b), the pump wave has been increased to $\alpha=0.01$. One of the sounds propagating forward has coupled to p_- to give rise to a decay process. This is an ordinary decay instability where the pump wave decays into a forward-propagating sound and a sideband wave. This corresponds to the first gap from the top. There is another gap, between (p_+,p_-). This is a nonresonant coupling in which the pump wave decays into two sideband waves. There is another gap at the origin between (p_+,e_-). This coupling corresponds to a modulational nonresonant instability. Moving to the right, there is another nonresonant instability, involving (e_-,p_-) [see Fig. 3(c)]. In Fig. 3(d) we have amplified the origin in order to show the modulational instability. Figures 3(b) and 3(c) are equivalent to Figs. 2(b) and 2(c), but ω_p has been increased by one order of magnitude and α has been decreased by one order of magnitude. Thus we observe that lower values of α are needed to destabilize the system for higher values of ω_p.

Next, we increase the sound velocity to $v_s/c=0.057$. For zero pump wave amplitude, the solutions of Eq. (32) are shown in Fig. 4(a). The crossings (S_+,p_+) and (S_-,p_-) have disappeared, and a new crossing (S_+,e_-) is present. There are five couplings in this case, as indicated in the figure. [Actually, the crossing (S_+,p_-) will not lead to coupling unless v_s is slightly less; we shall examine this later.] In Figs. 4(b) ($\alpha=0$) and 4(c) ($\alpha=0.001$), we see the crossing and then the coupling between (S_+,e_-), respectively. As in all previous decay processes, only one of the electroacoustic modes participates in the coupling. In Figs. 4(d) and 4(e) we show the crossing and the gap at the origin, respectively. Now S_+ is the rightmost line in the figure and the modulational instability is resonant, involving an electroacoustic mode and e_-. We have observed this same behavior for other sets of parameters: When v_s is so low that S_+ is to the left of p_+ and e_-, the modulational instability is nonresonant; when v_s is so high that S_+ is to the right of p_+ and e_-, the modulational instability is resonant. Next, in Figs. 5(a)–5(c), we show the other two possible gaps, between (p_+,p_-) and (e_-,p_-). Figure 5(a) shows the relevant zone for $\alpha=0$. In Fig. 5(b), $\alpha=0.005$, and the gap between (e_-,p_-) has developed, while the crossing (S_+,p_-) does not develop a gap. In Fig. 5(c), $\alpha=0.01$ and the gap (p_+,p_-) is now also visible.

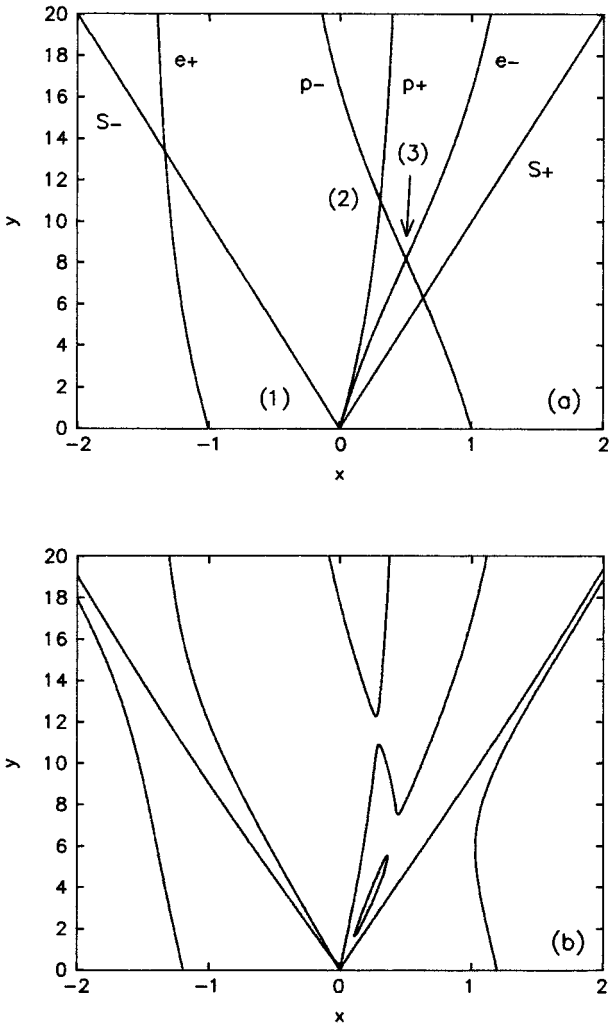

FIG. 7. Same as Fig. 3, but for $\omega_p/\omega_c=10$ and $v_s/c=0.1$. (a) $\alpha=0$. (b) $\alpha=0.08$.

Figures 6(a)–6(f) detail the evolution of the crossing (S_+,p_-). We have already shown in Fig. 3(b) that it leads to coupling between one electroacoustic mode and p_-, when $v_s/c=0.01$. In Fig. 6(a), v_s has been increased, but the crossing (S_+,p_-) is still to the left of the crossing (p_+,p_-). When $\alpha\neq 0$, Fig. 6(b), a gap still develops, but now the two electroacoustic modes are involved. In Fig. 6(c), v_s is further increased and the crossing (S_+,p_-) is to the right of the crossing (p_+,p_-). When $\alpha=0.01$, Fig. 6(d), a gap develops with both electroacoustic modes involved. Finally, Figs. 6(e) and 6(f) show this gap just before closing ($v_s/c=0.037$) and immediately after closing ($v_s/c=0.038$). It remains closed for higher values of v_s. The crossing (S_+,p_-) has always

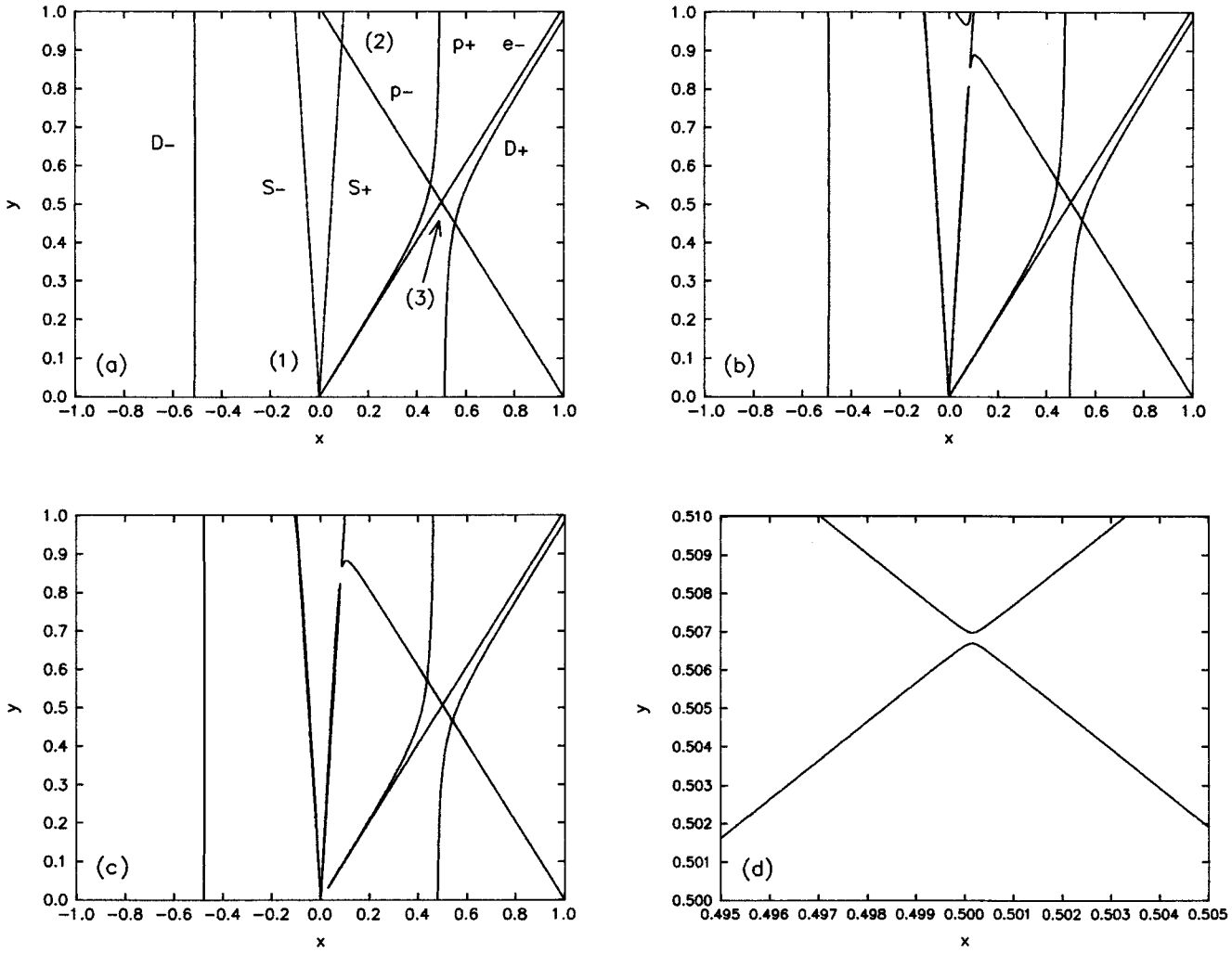

FIG. 8. Same as Fig. 3, for $\omega_p/\omega_c=0.1$ and $v_s/c=0.1$. (a) $\alpha=0$. (b) $\alpha=0.2$. (c) $\alpha=0.3$. (d) Enlargement of the region $x\simeq 0.5$ and $y\simeq 0.5$ of (c).

shown a similar behavior for the various sets of parameters we analyzed. The transition between a gap and an avoiding crossing always occurs when this crossing is in between the crossings (p_+,p_-) and (e_-,p_-).

Now we increase the sound velocity to $v_s/c=0.1$. Figure 7(a) corresponds to $\alpha=0$. We notice that the crossings (S_+,e_-) no longer exist and only three couplings are possible. These are shown in Fig. 7(b) for $\alpha=0.08$. From Fig. 7(b) it follows that there are two nonresonant couplings (p_+,p_-) and (e_-,p_-) and a resonant modulational instability between (S_+,e_-) at the origin.

In Fig. 8(a) we have reduced the plasma frequency to $\omega_p/\omega_c=0.1$. The other parameters are $v_s/c=0.1$ and $\alpha=0$. When ω_p decreases, the parabolic branches $D_\pm$ get closer, and therefore the crossings are the same as in Fig. 2(a), plus a new crossing, between (D_+,p_-). In Fig. 8(a) we have selected a region where all the crossings leading to wave coupling are present. The couplings are those expected, namely, an ordinary decay instability between (S_+,p_-), Fig. 8(b), a nonresonant modulational instability involving (e_-,p_+), Fig. 8(c), and a nonresonant coupling between (e_-,p_-), Fig. 8(d). The only new feature is the absence of a gap at the crossing (p_+,p_-). For all the values of ω_p we have studied, this crossing always leads to a coupling if v_s is low enough. This is the case for $\omega_p/\omega_c=1$ and $\omega_p/\omega_c=10$, where it develops a gap for $v_s/c\leqslant 0.48$ and $v_s/c\leqslant 0.42$, respectively.

We point out that we have also examined the intermediate cases $\omega_p/\omega_c=2$ and $\omega_p/\omega_c=0.5$. In the first case $\omega_p/\omega_c=2$, the threshold occurs for $v_s/c\simeq 0.47$, and in the second case $\omega_p/\omega_c=0.5$, it occurs for $v_s/c\simeq 0.53$. However, for $\omega_p/\omega_c=0.1$, there is never a gap at this crossing, even for v_s/c values as small as 10^{-6}.

V. SUMMARY

We have studied parametric decays of a circularly polarized wave in an electron-positron plasma, propagating in the direction of an external magnetic field. In general, there exist several instabilities, both resonant and nonresonant. The resonant instabilities are decay instabilities in which the pump wave decays into a forward-propagating electroacoustic wave and a sideband wave. The nonresonant instabilities are essentially electromagnetic, in which the pump wave decays into two sideband waves. Depending on the sound velocity and on the ratio ω_p/ω_c, there are two types of modulational instabilities. For $v_s/c\ll 1$, the modulational instability is nonresonant and gives rise to two sideband

daughter waves. For larger values of ω_p/ω_c, and if v_s/c is high enough, like, for example, the case of Fig. 4(a), the modulational instability is resonant and involves a forward propagating electroacoustic wave and a sideband wave.

The system is more sensitive to the pump wave amplitude for $\omega_p/\omega_c \gg 1$. As this ratio decreases, larger and larger amplitudes are needed in order to destabilize the system.

The particular case of pulsars magnetospheres corresponds to a situation in which $\omega_p/\omega_c \ll 1$, because of the existence of very strong magnetic fields. This case has been analyzed in Figs. 8(a)–8(d). In general, the type of instabilities involved are the same as in the other cases, except that instability ranges are smaller and larger pump wave amplitudes are needed to trigger the instabilities.

Notice that we have considered very small values of v_s/c because the treatment is valid only for nonrelativistic temperatures.

It is important to point out that, since our model is a fluid model, there are important effects, such as Landau damping and resonance absorption, that have not been considered. They can change the results and provide thresholds which are not present in our model. Therefore, a similar approach to the one used here, but using kinetic theory, is required.

ACKNOWLEDGMENTS

This paper was partially supported by FONDECYT, Grant No. 1960874, and Fundación Andes, Grant No. C-12999/6.

APPENDIX

Definitions for dispersion relation (32) are as follows:

$$F_{1+}=I_{+}+I_1\left(\frac{H_{p++}}{D_p}+\frac{H_{e++}}{D_e}\right)+\frac{1}{2}\,I_2\,\frac{H_{p0+}}{D_p}, \tag{A1}$$

$$F_{1-}=-\frac{1}{2}\,I_1\left(\frac{H_{p+-}}{D_p}+\frac{H_{e+-}}{D_e}\right)-\frac{1}{2}\,I_2\,\frac{H_{p0-}}{D_p}, \tag{A2}$$

$$F_{2+}=-\frac{1}{2}\,I_1\left(\frac{H_{p-+}}{D_p}+\frac{H_{e-+}}{D_e}\right)+\frac{1}{2}\,I_2\,\frac{H_{p0+}}{D_p}, \tag{A3}$$

$$F_{2-}=I_{-}+I_1\left(\frac{H_{p--}}{D_p}+\frac{H_{e--}}{D_e}\right)-\frac{1}{2}\,I_2\,\frac{H_{p0-}}{D_p}, \tag{A4}$$

$$I_{\pm}=c^2k_{\pm}^2-\omega_{\pm}^2, \tag{A5}$$

$$I_1=\omega_p^2, \tag{A6}$$

$$I_2=\omega_p^2 k k_0 c^2\left(\frac{eB}{mc^2k_0}\right)^2\left[\eta_p\left(1-\frac{1}{2}\,\alpha^2\eta_p^3\right)+\eta_e\left(1-\frac{1}{2}\,\alpha^2\eta_e^3\right)\right], \tag{A7}$$

$$D=[\omega_{+}(1+\alpha^2\eta^2)-\omega_c]\left\{-[\omega_{-}(1+\alpha^2\eta^2)-\omega_c]S+\frac{1}{2}\,\alpha^2c^2k_0^2\omega\,\frac{\omega_c}{\omega_0}\,\eta\left(1-\frac{1}{2}\,\alpha^2\eta^3\right)\right\}-\omega_{-}\,\frac{1}{4}\,\alpha^2\eta^2\left[-S\omega_{+}\alpha^2\eta^2\right.$$
$$\left.+\alpha^2c^2k_0^2\omega\,\frac{\omega_c}{\omega_0}\,\eta\left(1-\frac{1}{2}\,\alpha^2\eta^3\right)\right]+\frac{1}{2}\,\alpha^2c^2k_0^2\omega\,\frac{\omega_c}{\omega_0}\,\eta\left(1-\frac{1}{2}\,\alpha^2\eta^3\right)\left[\omega_{+}\,\frac{1}{2}\,\alpha^2\eta^2-\omega_{-}(1+\alpha^2\eta^2)+\omega_c\right], \tag{A8}$$

$$H_{++}=\omega_{+}\left\{-S[\omega_{-}(1+\alpha^2\eta^2)-\omega_c]+\frac{1}{2}\,\alpha^2c^2k_0^2\omega\,\frac{\omega_c}{\omega_0}\,\eta\left(1-\frac{1}{2}\,\alpha^2\eta^3\right)\right\}+\frac{1}{2}\,\alpha^2\omega\,\frac{\omega_c}{\omega_0}\,k_0k_{+}c^2\eta^2$$
$$\times\left(1-\frac{1}{2}\,\alpha^2\eta^3\right)^2\left[\omega_{+}\,\frac{1}{2}\,\alpha^2\eta^2-\omega_{-}(1+\alpha^2\eta^2)+\omega_c\right], \tag{A9}$$

$$H_{+-}=\omega_{-}\left[-\omega_{+}\alpha^2\eta^2S+\alpha^2c^2k_0^2\omega\,\frac{\omega_c}{\omega_0}\,\eta\left(1-\frac{1}{2}\,\alpha^2\eta^3\right)\right]+\alpha^2c^2k_0k_{-}\omega\,\frac{\omega_c}{\omega_0}\,\eta^2\left(1-\frac{1}{2}\,\alpha^2\eta^3\right)^2$$
$$\times\left[\omega_{+}\,\frac{1}{2}\,\alpha^2\eta^2-\omega_{-}(1+\alpha^2\eta^2)+\omega_c\right], \tag{A10}$$

$$H_{-+}=\omega_+\left\{-\omega_-\alpha^2\eta^2 S-\alpha^2c^2k_0^2\omega\,\frac{\omega_c}{\omega_0}\,\eta\left(1-\frac{1}{2}\,\alpha^2\eta^3\right)\right\}$$
$$+\alpha^2c^2k_0k_+\omega\,\frac{\omega_c}{\omega_0}\,\eta^2\left(1-\frac{1}{2}\,\alpha^2\eta^3\right)^2\left[-\omega_-\,\frac{1}{2}\,\alpha^2\eta^2+\omega_+(1+\alpha^2\eta^2)-\omega_c\right], \tag{A11}$$

$$H_{--}=\omega_-\left\{-S[\omega_+(1+\alpha^2\eta^2)-\omega_c]-\frac{1}{2}\,\alpha^2c^2k_0^2\omega\,\frac{\omega_c}{\omega_0}\,\eta\left(1-\frac{1}{2}\,\alpha^2\eta^3\right)\right\}$$
$$+\frac{1}{2}\,\alpha^2\omega\,\frac{\omega_c}{\omega_0}\,k_0k_-c^2\eta^2\left(1-\frac{1}{2}\,\alpha^2\eta^3\right)^2\left[-\omega_-\,\frac{1}{2}\,\alpha^2\eta^2+\omega_+(1+\alpha^2\eta^2)-\omega_c\right], \tag{A12}$$

$$H_{0+}=\omega_+\left[\omega_-\,\frac{1}{2}\,\alpha^2\eta^2+\omega_-(1+\alpha^2\eta^2)-\omega_c\right]-\frac{k_+}{k_0}\,\eta\left(1-\frac{1}{2}\,\alpha^2\eta^3\right)$$
$$\times\left\{[\omega_+(1+\alpha^2\eta^2)-\omega_c][\omega_-(1+\alpha^2\eta^2)-\omega_c]-\omega_-\omega_+\left(\frac{1}{2}\,\alpha^2\eta^2\right)^2\right\}, \tag{A13}$$

$$H_{0-}=\omega_-\left[\omega_+\,\frac{1}{2}\,\alpha^2\eta^2+\omega_+(1+\alpha^2\eta^2)-\omega_c\right]-\frac{k_-}{k_0}\,\eta\left(1-\frac{1}{2}\,\alpha^2\eta^3\right)$$
$$\times\left\{[\omega_+(1+\alpha^2\eta^2)-\omega_c][\omega_-(1+\alpha^2\eta^2)-\omega_c]-\omega_-\omega_+\left(\frac{1}{2}\,\alpha^2\eta^2\right)^2\right\}, \tag{A14}$$

$$S=\omega^2\left(1+\frac{1}{2}\,\alpha^2\eta^2\right)-v_s^2k^2. \tag{A15}$$

[1] P. K. Shukla, N. N. Rao, M. Y. Yu, and N. L. Tsintsadze, Phys. Rep. **138**, 1 (1986).
[2] A. Hewish, Annu. Rev. Astron. Astrophys. **8**, 265 (1970).
[3] T. V. Smirnova, Sov. Astron. Lett. **14**, 20 (1988).
[4] T. V. Smirnova, V. A. Soglasnov, M. V. Popov, and A. Yu. Novikov, Sov. Astron. **30**, 51 (1986).
[5] F. Curtis Michel, *The Theory of Neutron Stars Magnetospheres* (University of Chicago Press, Chicago, 1991).
[6] A. C.-L. Chian and C. F. Kennel, Astrophys. Space Sci. **97**, 9 (1983).
[7] R. E. Kates and D. J. Kaup, J. Plasma Phys. **41**, 507 (1989).
[8] F. T. Gratton, G. Gnavi, R. M. O. Galvão, and L. Gomberoff, Phys. Rev. E **55**, 3381 (1997).
[9] R. T. Gangadhara, V. Krishan, and P. K. Shukla, Mon. Not. R. Astron. Soc. **262**, 151 (1993).
[10] L. Gomberoff, V. Muñoz, and R. M. O. Galvão, Phys. Rev. E **56**, 4581 (1997).
[11] R. E. Kates and D. J. Kaup, J. Plasma Phys. **42**, 521 (1989).
[12] L. Gomberoff and R. M. O. Galvão, Phys. Rev. E **56**, 4574 (1997).
[13] K. Nishikawa and C. S. Liu, in *Advances in Plasma Physics*, edited by A. Simon and W. B. Thompson (Wiley, New York, 1976), Vol. 6, pp. 3–81.
[14] V. Muñoz and L. Gomberoff (unpublished).
[15] M. Longtin and B. U. Ö. Sonnerup, J. Geophys. Res. **91**, 6816 (1986).
[16] J. V. Hollweg, R. Esser, and V. Jayanti, J. Geophys. Res. **98**, 3491 (1993).
[17] R. M. O. Galvão, G. Gnavi, L. Gomberoff, and F. T. Gratton, Plasma Phys. Controlled Fusion **36**, 1679 (1994).
[18] L. Gomberoff, G. Gnavi, and F. T. Gratton, J. Geophys. Res. **100**, 17.221 (1995).
[19] G. Gnavi, R. M. O. Galvão, F. T. Gratton, and L. Gomberoff, Phys. Rev. E **54**, 4112 (1996).
[20] D. W. Forslund, J. M. Kindel, and E. L. Lindman, Phys. Rev. Lett. **29**, 249 (1972).